PAPER • OPEN ACCESS

Genesis and evolution of the Hamama volcanic massive sulphide deposits, Egypt

View the article online for updates and enhancements.

Genesis and evolution of the Hamama volcanic massive sulphide deposits, Egypt

A S Mahmoud[1*], V V Dyakonov[1] and A E Kotelnikov [2]

[1] Russian State Geological Prospecting University, Moscow, Russia
[2] Peoples' Friendship University of Russia (RUDN University), Moscow, Russia

E-mail: halim.geologist@mail.ru

Abstract. Hamama Zn-Pb-Cu VMS deposits are hosted along the contact of bimodal metavolcanic sequence and their volcaniclastics in association with quartz-carbonate matrix. Ore forming process include multi-stage steps. 3D interpolation of drill hole database shows that the ore body was affected by multidirectional faults and fracture zones, that later were occupied by carbonates. The origin of carbonates is approached using a C and O isotopic compositions in whole-rock samples. The isotopic data revealed signs of both hydrothermal-sedimentary and hydrothermal-metasomatic processes. The primary gold and sulphide minerals were deposited from exhalations, forming massive sulphide ore then the tectonic processes due to the emergence of two successive phases of granitoids followed by the of post-tectonic dykes provided war to the introduction of carbonates that changed the configuration of the ore deposit and affected its grade. Later diagenetic and metasomatic processes resulted in enrichment of gold in the oxidation zone.

1. Introduction

Volcanic massive sulphide (VMS) deposits are an interesting type of deposits for both by the miners and the geologists. They are not only a source of precious metals like gold and silver, but also base metals like Cu, Zn, Pb, and represent an important source of Co, Sn, Cd, Te, Bi, Mn, Gr, Ga and Ba. Some of them also contain trace amounts of Hg, Sb, Se, In, and As [1, 2], which save companies from the price fluctuation of the gold and silver. The Hamama VMS deposit, central Eastern Desert, Egypt, is one of several mineralized metavolcanic provinces in the Eastern Desert (ED). The prominent feature of this deposit is its association with carbonates. The Western Zone of Hamama is estimated to contain an indicated source of 137000 ounces and thus is considered one of Egyptian's promising gold resources [3]. However, the ore grade is lower than normal VMS deposits. Few data are available about the genesis ED VMS and their relation to associated carbonates. The obtained results significantly expand the current understanding of the genesis of the Hamama deposit and explain the causes of its low grade, which can be used in a comparative analysis with similar genetic type.

2. Materials and Methods

The field relationship of the host-rock metavolcanics, ore and carbonate were documented during two field trips. More than 100 thin polished sections were prepared for petrographic and mineralogical studies using transmitted-reflected light microscope. The drilling database of the company "Aton resources" representing analyses of 8440 drill hole samples and 4475 trench sample were used for 3D modelling and ore type classification. Seven samples picked manually from quartz-carbonate veins, nests and lenses from the Hamama deposit. The isotope analyses were carried out in the Institute of Geology of Ore Deposits, Petrography, Mineralogy and Biochemistry (IGEM- RAS), on a Deltaplus mass spectrometer (Thermo-Finnigan). Calibration in international scales V-PDB and V-SMOW was carried out using external (NBS-18, NBS-19, MCA-8) and laboratory (ATC-1) standards.

3. Results

3.1. Geology of the ore deposit

The Hamama area is occupied mainly by basic and intermediate metavolcanic rocks (meta-basalt, basaltic meta-andesite and meta-andesite) with pillow lava occupy the lower section (Figure 1). To the south, the metavolcanics are in contact with different types of volcaniclastic rocks (massive, lapilli and banded tuffs and breccia) intercalated with alternative bands of iron. Quartz carbonate veins occupy the contact of the metavolcanics and tuffs with different degrees of sulphide mineralizations forming a long channel of gossan on the surface. These carbonates can be divided into two types, a) non-mineralized, pure carbonate thin bands (1-15 cm thick); and b) mineralized thick layers of carbonates associated with sulphide mineralization (or oxides in the oxidation zone). The meta-basaltic sheet contains multiple felsic units, mainly meta-dacite and meta-rhyolite (Figure 1). The area was intruded by post-tectonic small quartz diorite dyke-like intrusion in the central part. A feldspar-quartz phyric rhyolite dyke extends in NE-SW direction, cutting the ore body, metavolcanics and volcaniclastics (Figure 1). Both acidic and basic metavolcanic rocks host extensive alteration zones around felsic metavolcanics and later granitoid bodies. The area was subjected to extensional tectonics resulted in the formation of a set of NW-SE strike-slip faults. Nubian sandstone (Cretaceous) covers the western and southern parts of the area with small outcrops.
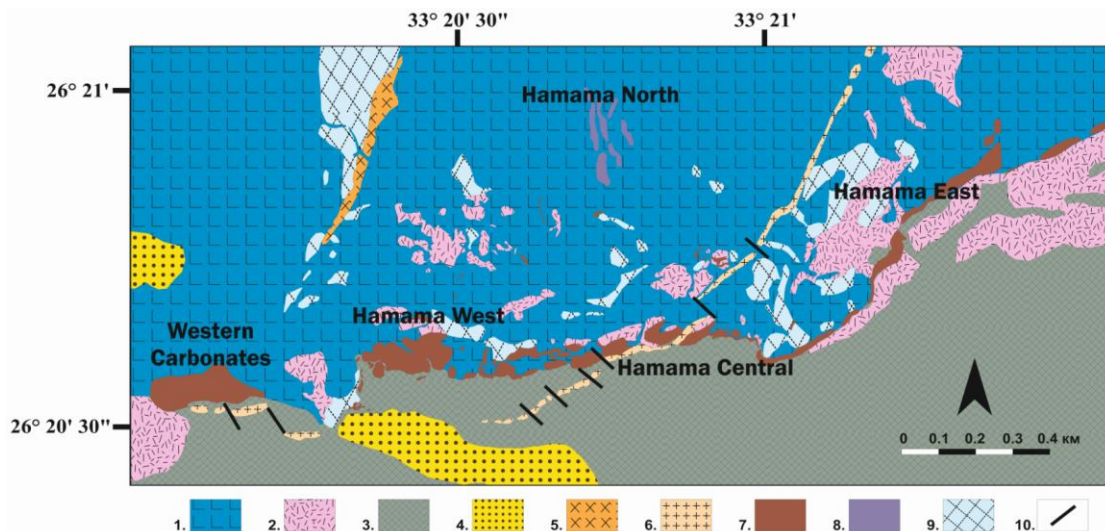

Figure 1. Geological map of the Hamama ore deposit. Legend: 1. Basic metavolcanics with pillow lava; 2. Acidic and intermediate metavolcanics; 3. Tuffs with banded iron formation; 4. Nubian sandstone; 5. Quartz diorite; 6. Rhyolite dykes; 7. Quartz-carbonate veins; 8. Quartz veins; 9. Alteration Zones; 10. Faults.

The metavolcanics, volcaniclastics and quartz-carbonate veins were exposed to long periods of tectonic deformation expressed by their large dipping angles. The drilling programs performed on the ore zones showed that the mineralized horizon is steeply dipping [4]. The stratigraphic sequence is overturned with dip ranges from sub-vertical to moderately overturned to the northwest, so the stratigraphic top is to the southeast [5].

3.2. Mineralogical characteristics and paragenesis

The ore samples are characterized by low to moderate sulphide mineralization (5-30%). Some drill cores revealed massive ore continuing up to 70 %. Mineralogically, it is composed in an average of about 30 % modal quartz with amorphous silica, 25% dolomite, 15% calcite, 10% pyrite, 10% other sulphides, 5% feldspar and clay minerals, and 5% chlorite with other constitutes. The overall identified ore minerals of the fresh ore are pyrite, sphalerite, chalcopyrite, galena, and covellite, with varying amounts of cinnabar, arsenopyrite, stibnite, enargite, iodargyrite, greenockite, acanthite, and

tetrahedrite. The oxide equivalents include hematite, goethite, limonite, zincite, and litharge. Sampled fresh ore from drill cores can be distinguished into two groups: a. Pyrite-rich (Figure 2a-f), and b. Polymetallic sulphides (Figure 2g, h). The pyrite-rich ore is the most common type. In terms of massiveness, the ore can be divided into two types: a) vein and disseminated ores, containing low-thickness veins of ores, as well as interlayers of poorly mineralized disseminations of pyrites, with other sulphides in small quantities. b) Massive ore with more than 30 % of ore minerals (Figure 2g, h). Sphalerite is the main ore mineral in this type, followed by pyrite, chalcopyrite, and galena.
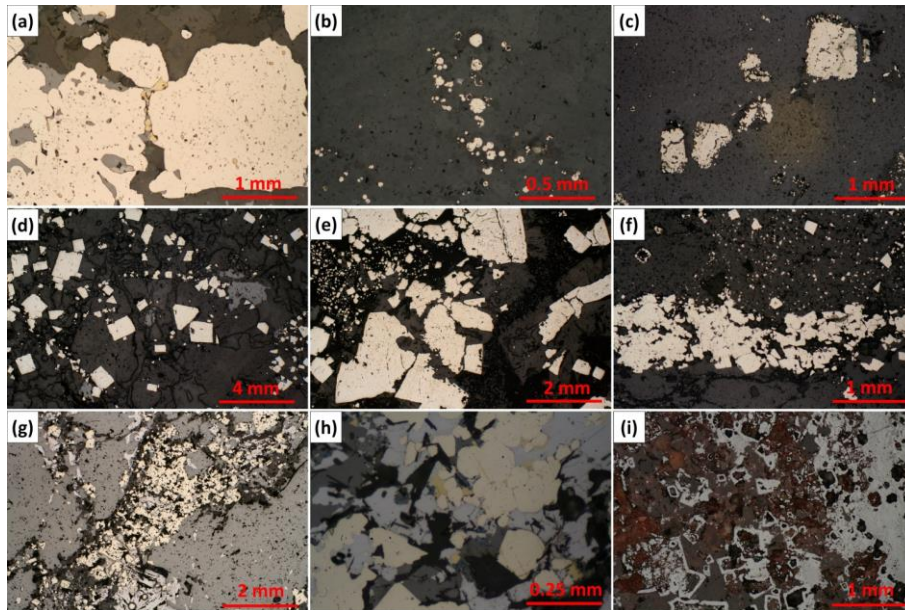
Figure 2. a) chalcopyrite filler between Py-1 grains, which contains inclusions of sphalerite; b) Fine pyrite framboids (Py-2), c) Reserved nests of framboid bacteria built on (Py-1) pyrite cubes; d) fine grained pyrite (Py-3) and sphalerite deposited along carbonate boundaries; e) coarse, fractured grains of py-1 and fine-grained py-3 in the highly altered parts; f) vein of pyrite (Py-1) and fine scattered (Py-3); g) inclusions of galena and pyrite in sphalerite; h) inclusion of pyrite, and chalcopyrite (replaced partially to covellite) in tetrahedrite and sphalerite; i) alteration products of sulphide mineralizations preserving cube form of pyrite.

Table 1. Paragenetic sequence of hydrothermal and supergene stages of the Hamama deposit.

Mineral	Hydrothermal stage			Supergene stage
	Pre-ore step	Ore step	Post-ore step	
Carbonates		▬▬▬▬▬▬▬▬▬		
Quartz	▬▬▬▬▬			
Pyrite	▬▬▬▬▬	▬▬▬▬▬	▪ ▪ ▪ ▪ ▪ ▪	
Feldspar	▬▬▬			
Chlorite	▪ ▪ ▪ ▪ ▪ ▪			
Sericite	▪ ▪ ▪ ▪ ▪ ▪ ▪ ▪ ▪ ▪ ▪ ▪ ▪			
Sphalerite	▬▬▬▬			
Goethite				▬▬▬▬▬
Talc		▪ ▪ ▪ ▪ ▪ ▪ ▪ ▪ ▪ ▪ ▪ ▪ ▪		
Chalcopyrite	▬▬▬			
Galena	▪ ▪ ▪ ▪ ▪ ▪			
Covellite			▪ ▪ ▪ ▪ ▪ ▪	
Barite			▬▬▬▬▬▬	
Tetrahedrite	▪ ▪ ▪ ▪ ▪			
Mineral abundance:	▬▬▬ Major,	▬▬▬ Minor,	▪ ▪ ▪ ▪ ▪ Rare	

The process of ore formation was rather complex, expressing signs of both hydrothermal-sedimentary and hydrothermal-metasomatic processes. The hydrothermal and supergene stages of the ore formation are represented in (table 1) discussed below:

3.2.1. The pre-ore step is represented by dissemination of the ore minerals with the hosting rock-forming minerals and their alteration products. The mineral assemblage of this stage is represented by plagioclase, amorphous silica, quartz, calcite, barite, chlorite, sericite, kaolin, pyrite (Py-0), few galena, sphalerite and chalcopyrite. The mineral assemblage of this stage is preserved mainly in the stringer zone in the hanging wall tuffs and carbonate lenses.

3.2.2. The ore step includes the intensive deposition of ore minerals include, in descending order, pyrite (Py-1), sphalerite, galena and chalcopyrite (Cpy-1), secondary - pyrrhotite, less common - arsenopyrite, enargite, greenockite, cinnabar, acanthite; nonmetallic minerals - quartz, calcite, dolomite, barite, chlorite, sericite, kaolinite. The mineral assemblage of this stage can be observed mainly in the massive ore from deep drill cores of the Hamama western zone.

3.2.3. The post-ore step expresses the formation of most carbonate mass and reworking of ore minerals producing some secondary sulphide minerals in the fresh ore chiefly of copper as covellite, bornite, chalcopyrite (Cpy-2), and tetrahedrite. It also includes the formation of new generations of pyrite as framboids (Py-2) and fine skeletal grains (Py-3) related to alteration of host rock.

3.2.4. The supergene stage includes the formation of secondary minerals of oxides and carbonates as hematite, goethite, limonite, acanthite, zincite, litharge, malachite, siderite, smithonite, otavit, anglesite, and rare native gold etc.

Four generations of pyrite are distinguished. Pyrite-0 represents the primary well-crystallized pyrite as inclusions in early sphalerite and galena (Figure 2h) and encountered in the massive ore. Pyrite-I composes the main mass of pyrite. Grains of pyrite-1 contain inclusions of non-metallic minerals, cracked, often coarse (up to 1.5 mm), anhedral crystals, crushed to fine-grained aggregates (Figure 2a, c, d, e). Chalcopyrite, galena, sphalerite, are partially replaced grains of pyrite-1. Framboidal pyrite represents the pyrite-2 that formed by bacterial action in reducing environment. There are also clusters of individual, framboids, cemented by non-metallic minerals (Figure 2b, c). They subjected to many reworking processes producing new forms include atoll-like pyrite. Pyrite-3 occurs as idiomorphic crystals without inclusions of other minerals and cracks. Pyrite-III grains are very fine; from thousandths to hundredths parts of a mm; form chains, or uniform disseminations in ores (Figure 2d, e, f). Sphalerite is, generally, found in a subordinate amount, except in massive ore may exceed 70 vol. %. It is found in the form of complex intergrowths or as "independent" xenomorphic grains (aggregates). Independent grains contain almost no inclusions of sulphides and non-metallic minerals and has curly boundaries corroded by carbonates. Sphalerite formed during the first stage of ore formation. A characteristic feature of the earlier sphalerite is emulsion-like inclusions of chalcopyrite rarely exceed 0.1 mm in size. Chalcopyrite occurs in the form of xenomorphic grains in accretion with ore-forming sulphides and in the form of emulsifying impregnation in sphalerite (Cpy-1), and forms late veins in the sphalerite-pyrite association. Chalcopyrite-1 (Figure 3h) most often occurs with sphalerite in the composition of xenomorphic-grained clusters, and confined to the intergranular spaces of pyrite and fills cracks in them. Chalcopyrite-2 (Figure 3a) is emulsion-like inclusions in sphalerite but probably later xenomorphic clusters and intergranular fillings, indicating that after the deposition of the main mass of sphalerite, the flow of copper-bearing ore-forming solutions did not stop. Galena occurs in the form of inclusions and deformed veins within large sphalerite masses. The spatial relationships of galena with pyrite, sphalerite indicates that the deposition of galena began later, but without a temporary interruption in ore formation.

3.3. Ore classification

Different diagrams for classification of VMS were used to define the type of the ore deposit using the database of "Aton resources" of the fresh ore sample. In terms of gold, silver and base metal contents (Cu+Zn+Pb), the majority of the ore samples (>70 %) fall in the field of base metal deposits (Figure 3a), rather than the gold deposits [6-8]. However, some ore samples fall in the field of auriferous

deposits due to its relatively high silver contents rather than gold contents. The average point falls in the field of base metal deposits.
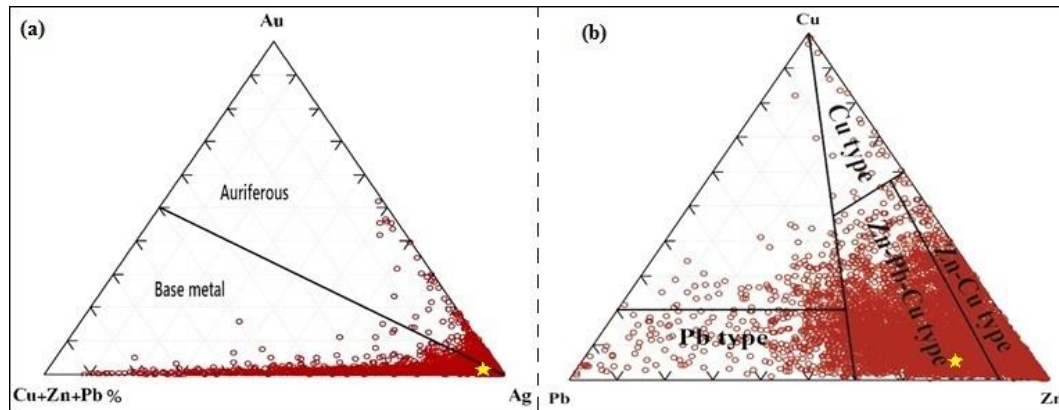
Figure 3. a) Ternary representation of the relative abundances of Au (ppm), Ag (ppm), and base metal (%) in the Hamama deposit [7] ; b) Ternary representation of the relative abundances of Cu, Zn and Pb in the Hamama deposit [9]; the average values in both plots are represented by a star.
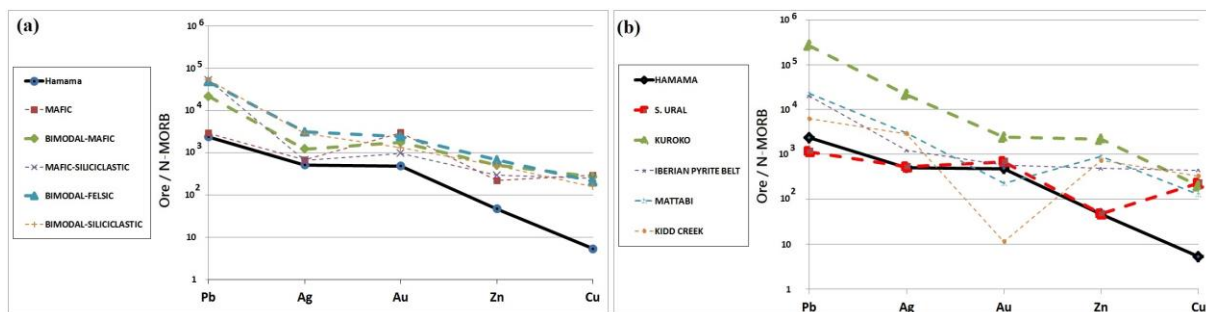
Figure 4. N-MORB normalized diagrams for average Pb, Ag, Au, Zn and Cu contents for the Hamama deposits (solid line) compared pattern with type of host rock (a) and common VMS types (b); values for N-MORB normalization and VMS host-rock types from [10, 11] ; for Sibai of South Ural from [12]; for Kuroko-type, Uchnotai, Kosaka mine, Japan from [13] ; for Kid Creek, Timmins District, Canada from [14] ; for Rio Tinto, Iberian Pyrite Belt, Spain from [15] .

The Hamama deposit belongs to Zn-Pb-Cu type (> 70 % of samples) as revealed from the ternary plot of [9] , where about 20 % fill in the field of Zn-Cu type, the remaining part fills the field Pb type with few samples fall in the Cu type (Fig. 3b). Correlation of N-MORB normalized metal contents of Hamama deposits based on host rock shows a strong correlation with bimodal felsic and bimodal mafic host rock VMS (Fig. 5a). In fact, the Hamama deposit is hosted in bimodal mafic sequence, but silicification of the deposit resulted in its higher correlation with bimodal felsic host for VMS. Correlation of N-MORB-normalized metal content of Hamama with common VMS types (Fig. 4b) shows that Hamama deposit correlates strongly with Kuroko-type and South Ural pyrite deposits (Sibai) and share some similarities with Kid Creek, Mattabi and Iberian Pyrite Belt (Fig. 5b). Hamama agrees with Kuroko-type in that both of them are Zn-Pb-Cu type. However, metal contents of all metals of Hamama are lower. Also, Hamama is more comparable to Sibai Cu-Zn pyrite [16] deposit of South Ural in metal contents except for copper where Sibai has higher copper concentrations.
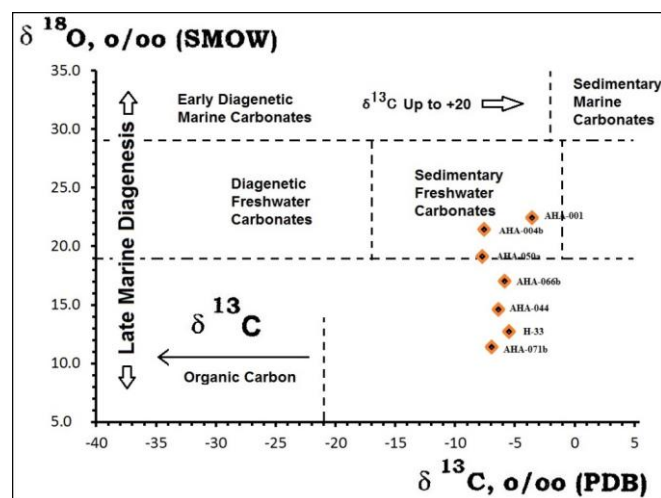
3.4. C and O isotopic compositions of carbonates
Carbonation is a very common feature associated with green-schist facies metamorphosed metavolcanics of the Eastern Desert. Stern and Geinn [17], stated that large amounts of carbonate having been added to the basement during deformation and metamorphism. The origin, age of formation and the relation of these carbonates to mineralization is not clear. Seven samples picked

manually from quartz-carbonate rock, manifest a diverse mineralogy. Mineralogical investigation indicates that these samples consist of calcite (H-33, AHA-050a, AHA-066b, AHA-071b), dolomite + calcite (AHA-004b, AHA-044), and calcite + smithsonite + dolomite (AHA-001). The C, and O isotopes of the carbonate samples cluster between -7.68‰ and -3.55‰ for $\delta^{13}C$ (delta-C-18) (average= - 6.26), and +11.45‰ and +22.37‰ (average= 16.94) for $\delta^{18}O$ (delta-O-18) (Table 2). The $\delta^{13}C$ isotopic signature of the carbonates from Hamama area are consistent with the value of the mantle derived rocks, ($\delta^{13}C \sim -5$ to -6 ‰; [18-20] . Such a low value is usually could be taken to signify an absence of life, since photosynthesis usually acts to raise the value. Biological materials on the one hand are strongly depleted in $\delta^{13}C$ (- 20 to - 30 ‰; the mean value of the terrestrial biomass is - 26 ± 7 ‰ according to [21].

Table 2. The carbon and oxygen isotope contents of the separated carbonates, Hamama deposits. V-PDB: Vienna Pee Dee Belemnite standard and V-SMOW: Vienna Standard Mean Ocean Water.

| Sample	Carbonate content in the sample, wt. %	$\delta^{13}C$ (V-PDB)	^{13}C (Stand. Dev.)	$\delta^{18}O$ (V-SMOW)	^{18}O (Stand. Dev.)
H-33	73	-5.54	0.04	12.59	0.06
AHA-001	99	-3.55	0.04	22.37	0.06
AHA-004b	101	-7.61	0.04	21.42	0.06
AHA-044	48	-6.38	0.04	14.54	0.06
AHA-050a	121	-7.68	0.04	19.18	0.06
AHA-066b	105	-5.91	0.04	17.03	0.06
AHA-071b	65	-6.94	0.04	11.45	0.06

Figure 5. O and C isotopic composition of the Hamama carbonates on the Kuleshov diagram [22].

Our $\delta^{18}O$ values (from 11.45‰ to +22.37) are in agreement with the previous work of Stern and Gwinn [17] ($\delta^{18}O$ from +9.5 to + 27.4‰), carried on samples from the Central Eastern Desert of Egypt. They explained the origin of the "intrusive" carbonates of the Central Eastern Desert as mixing between remobilized sedimentary carbonates and mantle fluids of low temperatures (< 300 ° C). This inference is also consistent with the lack of any evidence for chilled margins on any of the carbonate veins. In the diagram of Kuleshov [22]   (Fig. 5), three samples fill in the field of sedimentary fresh water carbonates which have $\delta^{18}O$ (V-SMOW) > 19. It is noticed that these three samples are reworked. Thus, their higher values of ^{18}O are due to further addition from meteoric water upon alteration. These results suggest occurring of some isotopic re-equilibration with a lower temperature fluid, and probably the involvement of metasomatic fluids.

3.5. 3D interpolation of drill holes database

The results of 3D interpolation of the database (Fig. 6) of Hamama deposits shows that the ore body is about 3 km length, up to 110 m thick, more than 250 m deep, and steeply-dipping with an average angle of 55 ° to the south.
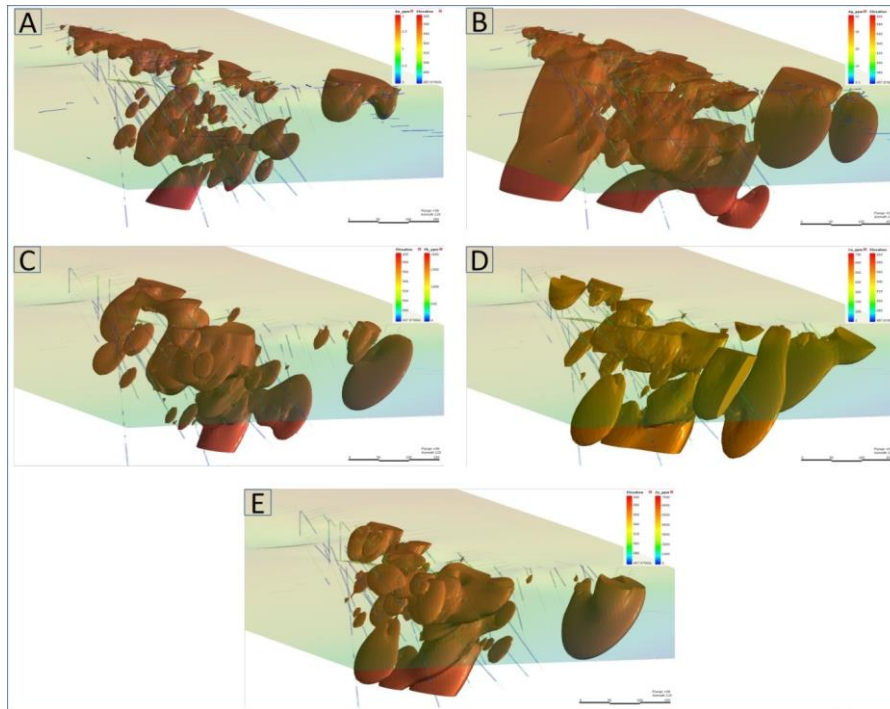
Figure 6. 3D model for distribution of Au, Ag, Pb, Cu, and Zn respectively in Western Hamama.

The high-grade ore of the Hamama West is separated into small pieces and not grouped into a continuous ore body. It is controlled by multidirectional faults and fracture zones. These faults formed after the complete formation of the ore body and strongly changed its configuration. The Hamama East appears on the surface as isolated masses dissected by many strike-slip faults due to its closest from centre of tectonic activity. In the central Hamama, the ore body is crossed by a large rhyolitic dyke, and then this dyke is dissected into small masses by a set of strike-slip faults (Figure 1). In many places, these strike-slip faults are filled with quartz-carbonate rock. The carbonates have apophasis in the surrounding metavolcanics, which increases the indication of their hydrothermal origin.

4. Discussion

Geochemically, the Hamama ore are classified as Zn-Pb-Cu (polymetallic) VMS type. However, its metal content is lower than normal VMS provinces. The field observations indicate that the Hamama VMS were exposed to long-period of tectonics. The 3D interpolation of drilling database supports this observation, where the cut-off grade is bothered and separated into small masses. The ore mineralization is hosted in carbonate matrix.   The crosscutting relationship suggests that carbonatization post-dated silicification. The C and O isotope compositions support the hydrothermal origin of these carbonates. The restriction of carbonate in areas of tectonic disturbance refers to their late formation. The introduction of the carbonate that lowered the ore grade was probably contemporary to the emergence of granitoids.

Conclusions

The Hamama deposits are steeply dipping ore body classified as bimodal Zn-Pb-Cu VMS deposit. Paragenetic sequence of ore and gangue minerals is given. Mineralogical investigations indicate that

carbonate formed in later stages after ore formation. Isotopic compositions of carbonate gangue indicate hydrothermal origin and signs of reworking by later low temperature fluids. 3D model of metal contents shows that the ore body is dissected into small parts. The introduction of two phases of granitoids in the eastern and northern parts of the Hamama area, in addition to the emergence of post-tectonic dikes, played an important role in changing the configuration of the ore deposit. The formation of the Hamama deposit included three steps: a. Formation of Kuroko type VMS ores similar to modern black smokers; b. The ore body was dissected by a series of faults, and fractures. Ore became brecciated and cemented by silicates and c. The ore body then was subjected to a new tectonic stage with the introduction of a high-alkaline hydrothermal solution, filling cavities and newly formed cracks by carbonates.

References

[1] Allen R L and Weihed P 2002 *Geological Society*, London, Special Publications **204(1)** pp 13-37

[2] Hannington M, Barrie C and Bleeker W 1999 *The gaint Kidd Creek volcanogenic massive sulfide deposit, western Abitibi Subprovince, Canada* (Canada: Economic Geology Publishing Company) pp 616-72

[3] Aton Resources 2017 Independent technical report, Hamama West deposit, Abu Marawat concession, Arab Republic of Egypt 24 January 2017 *Cube Consulting* NI 43-101 p 121

[4] Alexander Nubia 2014 Summary note 7th january 2014 *Vicarage capital limited* **2** URL: https://www.js-research.de/fileadmin/user_upload/aan_vcl.pdf

[5] Alexander Nubia 2012 Technical report on the Abu Marawat concession, Egypt April 5, 2012 *Roscoe Postle Associates Inc.* NI 43-101 Report 112 URL: https://www.atonresources.com/site/assets/files/1201/abu_marawat_43-101.pdf

[6] Hannington M, Kjarsgaard I and Bleeker W 1999 *Economic geology Monograph* **10** p 61

[7] Poulsen H and Hannington M 1995 *Geology of Canadian mineral deposit types, geology of canada* **8** pp 183-96

[8] Poulsen K H 2000 *Bulletin of the geological survey of canada* **540** p 106

[9] Large R R 1992 *Economic geology* **87(3)** pp 471-510

[10] Barrie C and Hannington M 1999 *Reviews in economic geology* **8** pp 2-10

[11] Galley A G, and Koski R A, 1999, Setting and characteristics of ophiolite-hosted volcanogenic massive sulfide deposits, in Barrie C T, and Hannington M D 1999 *Reviews in Economic Geology* **8** pp 215-36

[12] Galley A G, Hannington M D and Jonasson I 2007 Volcanogenic massive sulphide deposits. Mineral deposits of canada: a synthesis of major deposit-types, district metallogeny, the evolution of geological provinces, and exploration methods: geological association of canada, mineral deposits division, special publication **5** pp 141-61

[13] Oshima T 1974 *Mining geol spec issue* **6** pp 89-100

[14] Franklin J and Thorpe R 1982 *Spec pap geol assoc can.* **25** pp 3-90

[15] Leistel J, et al. 1997 *Mineralium deposita* **33(1-2)** pp 2-30

[16] Prokin V A 1977 *Patterns of distribution of pyrite deposits in the South Urals* (Moscow: Publishing House Nedra)

[17] Stern R J and Gwinn C J 1990 *Precambrian research* **46(3)** pp 259-72

[18] Deines P 1980 *Handbook of environmental isotope geochemistry* (Chapter 9 - The isotopic composition of reduced organic carbon) Elsevier **1** pp 329-406

[19] Exley R, Mattey D, Clague D and Pillinger C 1986 *Earth and planetary science letters* **78(2-3)** pp 189-99

[20] Pineau F, Javoy M and Bottinga Y 1976 *Earth and planetary science letters* **29(2)** pp 413-21

[21] Schidlowski M 1987 *Annual review of earth and planetary sciences* **15(1)** pp 47-72

[22] Kuleshov V 2001 *Lithology and Mineral Resources* **36(5)** pp 429-44